Korean J. Chem. Eng., **28**(9), 1927-1935 (2011)
DOI: 10.1007/s11814-011-0044-2

Effects of sodium dodecyl benzenesulfonic acid (SDBS) on the morphology and the crystal phase of $CaCO_3$

Dae Ju Hwang*,**, Kye Hong Cho*, Moon Kwan Choi*, Young Hwan Yu*, Seung Kwan Lee*, Ji Whwan Ahn**, Gwang Il Lim***, Choon Han***,†, and Jong Dae Lee****

*Korea Institute of Limestone and Advanced Materials, 63, Wooduk-ri, Maepo-up, Danyang-gun, Chungbuk 395-903, Korea
**Mineral Processing Department, Mineral Resources Research Division,
Korea Institute of Geoscience and Mineral Resources, 92-Science-ro, Yuseong-gu, Daejeon 305-350, Korea
***Department of Chemical Engineering, Kwangwoon University, 447-1 Wolgye-dong, Nowon-gu, Seoul 139-701, Korea
****Department of Chemical Engineering, Chungbuk National University,
410 Sungong-ro, Heungduk-gu, Chung-ju, Chungbuk 361-763, Korea
(*Received 21 December 2010 • accepted 20 February 2011*)

Abstract–The effects of anionic surfactant on the morphology and crystallization of calcium carbonate precipitated from $CaCl_2$ and Na_2CO_3 were investigated. Although reaction temperature did not have an effect on the morphology of calcium carbonate, it did have an effect on the cluster size. The cluster size became bigger with high reaction temperature. With the addition of sodium dodecyl benzenesulfonic acid (SDBS), the morphology of precipitated calcium carbonate changed from cubic to porous spheres with over 98% of the crystal phase transformed from calcite to vaterite. The analysis of precipitates formed by the reaction of $CaCl_2$ solution (from limestone (CaO 50% content)) and Na_2CO_3 found that the morphology of precipitated calcium carbonate changed from cubic to spherical, and the crystal phase changed from calcite to over 94% vaterite with the addition of sodium dodecyl benzenesulfonic acid. These vaterite structures were solid spheres rather than hollow ones.

Key words: Calcium Carbonate, Anionic Surfactants, Calcite, Vaterite, Drug Delivery System

INTRODUCTION

Calcium carbonate ($CaCO_3$) has calcite, aragonite and vaterite crystal structures, with calcite the most stable. In natural conditions, vaterite is thermally unstable, and thus is easily re-crystallized to calcite [1-4]. To control calcium carbonate crystallization, $Ca(OH)_2$-CO_2-H_2O systems and $CaCl_2$-Na_2CO_3 system are used. In the former, controlling the phase of calcium carbonate is difficult, first because of the ductility factor of limestone during calcining for 1 to 2 hours at 1,000 °C in a kiln, and second because lime milk ($Ca(OH)_2$) is manufactured by the hydration of CaO. Cubic, calcite calcium carbonate usually then forms from the lime milk and CO_2 due to the effects of SiO_2, MgO, Fe_2O_3, Al_2O_3 impurities in the limestone and the reaction with lime milk [5]. A kiln's fuel differs depending on the kiln type, which affects CaO morphology [6]. Therefore, the formation of vaterite structures in calcite is studied through controlling $CaCl_2$-Na_2CO_3 systems [7-9].

The crystal structure of $CaCO_3$ can be controlled by additives in the $CaCl_2$-Na_2CO_3 system. Polymorphs of $CaCO_3$ can be produced by forming chains of Ca^{2+} and CO_3^{2-} ions in organic media [10]. Vaterite $CaCO_3$ with spherical structures is thermally stable in aqueous solutions and is synthesized with organic acid additives [11-16]. Also, spherical vaterite $CaCO_3$ can be synthesized by adding amino acids in bio-mineralization systems [17,18]. Polymorphous $CaCO_3$ can also be synthesized with inorganic additives [19] or enzymes [20,21].

Encapsulation through self-assembly can coat functional substances with outer layers, with variously sized macro-, micro-, or nano capsules and also multilayer capsules possible. Encapsulation protects the inner material from the outside environment, and thus protects it from oxidation and other degradation, maintaining its capability and stability. Encapsulation also facilitates the coated substance's application in various systems by controlling its release through the coating substance that can be chosen for its behavior in various environments [22-25].

Recently, porous spherical vaterite $CaCO_3$ has been synthesized by layer-by-layer (LBL) self-assembly encapsulation and applied to drug delivery systems (DDS). Shape and crystallization can be controlled through the use of additives during calcium carbonate growth in layer-by-layer self-assembly systems. Such systems can be used to control the release of such as proteins, antibiotic and anticancer agents with the use of anionic PSS (poly(sodium 4-styrenesulfonate)) and cationic PAH (poly(allylamine hydrochloride)) electrolytes [26-37].

Vaterite $CaCO_3$ has been studied though adding SDBS, an anionic surfactant similar to the anionic electrolyte PSS, to $CaCl_2$-Na_2CO_3 systems [38-41,43-46]. According to the studies, hollow-type vaterite $CaCO_3$ could be synthesized by adding commercial $CaCl_2$.

This work aimed to synthesize vaterite $CaCO_3$ of solid spheres rather than hollow ones. For the purpose, the anionic surfactant and $CaCl_2$ solution through the Solvay process with the use of lime-

†To whom correspondence should be addressed.
E-mail: chan@kw.ac.kr

stone (CaO, 50%) were employed instead of commercial $CaCl_2$.

EXPERIMENTAL

1. Materials and Characterization

$CaCl_2$ of purity >74%, MW 110.99 was supplied by OCI Company, Korea. Na_2CO_3 of purity >99.2%, MW 116 was supplied by OCI Company, Korea and used without further purification. Limestone with 50% CaO content was supplied by BeakKwang Mineral Material Co. Ltd., Korea. The anionic surfactant was SDBS (sodium dodecyl benzenesulfonic acid 50%, $C_{12}H_{25}C_6H_4SO_3Na$, JUNSEI, MW 348.48). HCl and NaOH (OCI company, Korea) of 98% purity were used.

The crystal shape and quantity of $CaCO_3$ were analyzed by an x-ray diffraction system (D/MAX2500V/PC, Rigaku, Japan) with maximum power 18 kW, voltage 60 kV, current 300 mA, and Cu/K-alpha radiation. Particle size of $CaCO_3$ was measured by the particle size analyzer (LS13320, Beckman Coulter, U.S.A.). A field emission scanning electron microscope (FE-SEM model: S-4300, HITACHI, Japan) was used to analyze the microstructure and shape of the $CaCO_3$. CaO content of the limestone was analyzed by an x-ray fluorescence spectrometer (ZSX Primus II, Rigaku, Japan). The purity of $Ca(OH)_2$ was analyzed by adding NaOH (2 mol) to the manufactured $CaCl_2$. The vibrational frequencies of the CO_3^{2-} ions of the synthesized $CaCO_3$ were analyzed by Fourier transform infrared spectrometry (FT-IR, Vertex 70, Bruker Optics, Germany).

2. Syntheses of $CaCO_3$

2-1. Without Anionic Surfactant

Samples a, a-1, a-2 and a-3 were formed from equimolar portions of $CaCl_2$ and Na_2CO_3 agitated for 1 hour at pH=9. The samples were thrice washed with distilled water and then dried for 12 hours at 70 °C. The four samples were synthesized at room temperature, 40 °C, 60 °C, and 80 °C, respectively (Fig. 1).

2-2. With Anionic Surfactant

Samples b, b-1, b-2, b-3 and b-4 were similarly formed from equimolar portions of $CaCl_2$ and Na_2CO_3 agitated for 1 hour at pH= 9. They too were thrice washed with distilled water and dried for 12 hours at 70 °C. The samples' molar SDBS contents relative to either $CaCl_2$ or Na_2CO_3 were 0.3%, 0.1%, 1%, 50% and 100% respectively (Fig. 1).

2-3. With Anion Surfactant using Limestone

Limestone (CaO content 50%) was pulverized to 2-5 mm and further diminished by a water mill. 125 μm particles were used after sieving. After reacting 1 kg limestone powder with 6 M HCl, pure $CaCl_2$ solution was produced by two cycles of filtering through glass fiber. Reacting a 1 : 1 : 1 molar ratio of Na_2CO_3, SDBS and the $CaCl_2$ solution produced $CaCO_3$ (sample b-5). Sample b-6 $CaCO_3$ was similarly synthesized but without the surfactant. The impurities of the $CaCl_2$ solution were assayed by synthesizing $Ca(OH)_2$ (sample b-7) with a 1 : 2 molar ratio of $CaCl_2$ and NaOH (Fig. 1).

RESULTS AND DISCUSSION

1. The Effect of Temperature on $CaCO_3$ Synthesis

The crystallization of $CaCO_3$ polymorphs in the $CaCl_2$-Na_2CO_3 system can be controlled by pH, the presence of additive and seed, temperature, and concentrations/super-saturation [7-9].

In this study, the effects of temperature on the $CaCl_2$-Na_2CO_3 system without surfactant were tested (Fig. 1). Eq. (1) describes the system's reaction.

$$CaCl_2+Na_2CO_3 \rightarrow CaCO_3+2NaCl \quad (1)$$

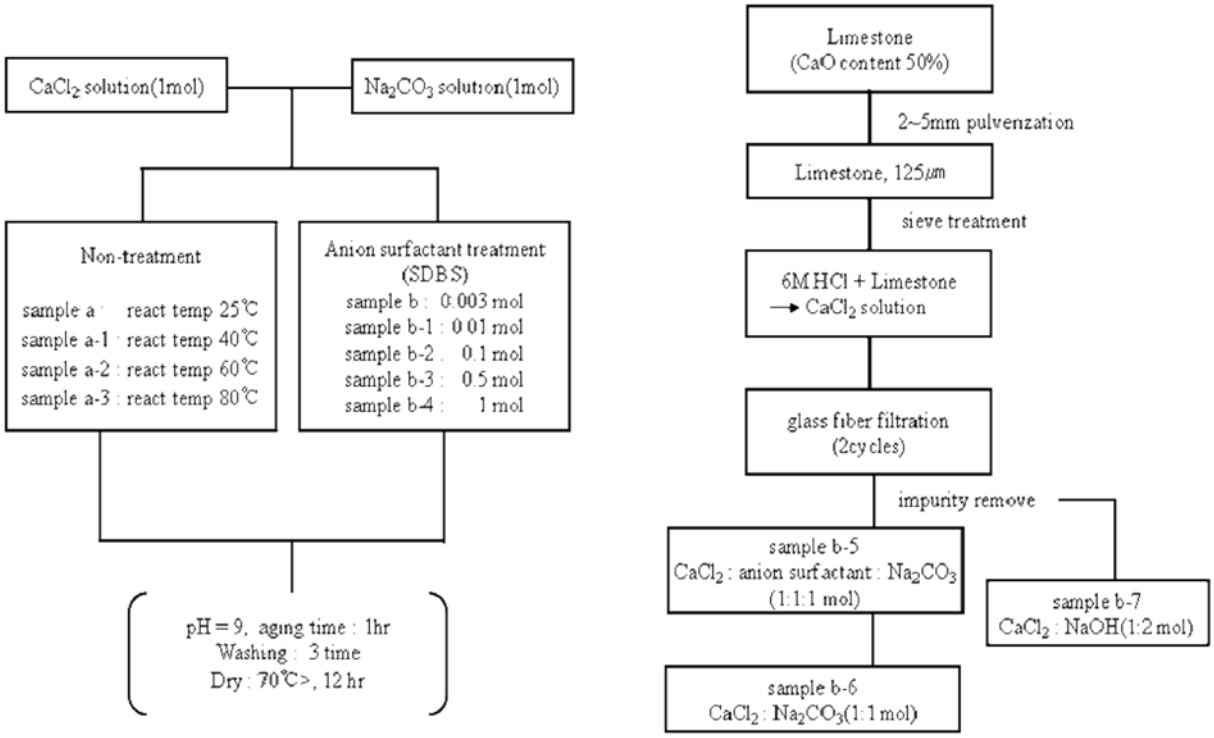

Fig. 1. Syntheses of $CaCO_3$.

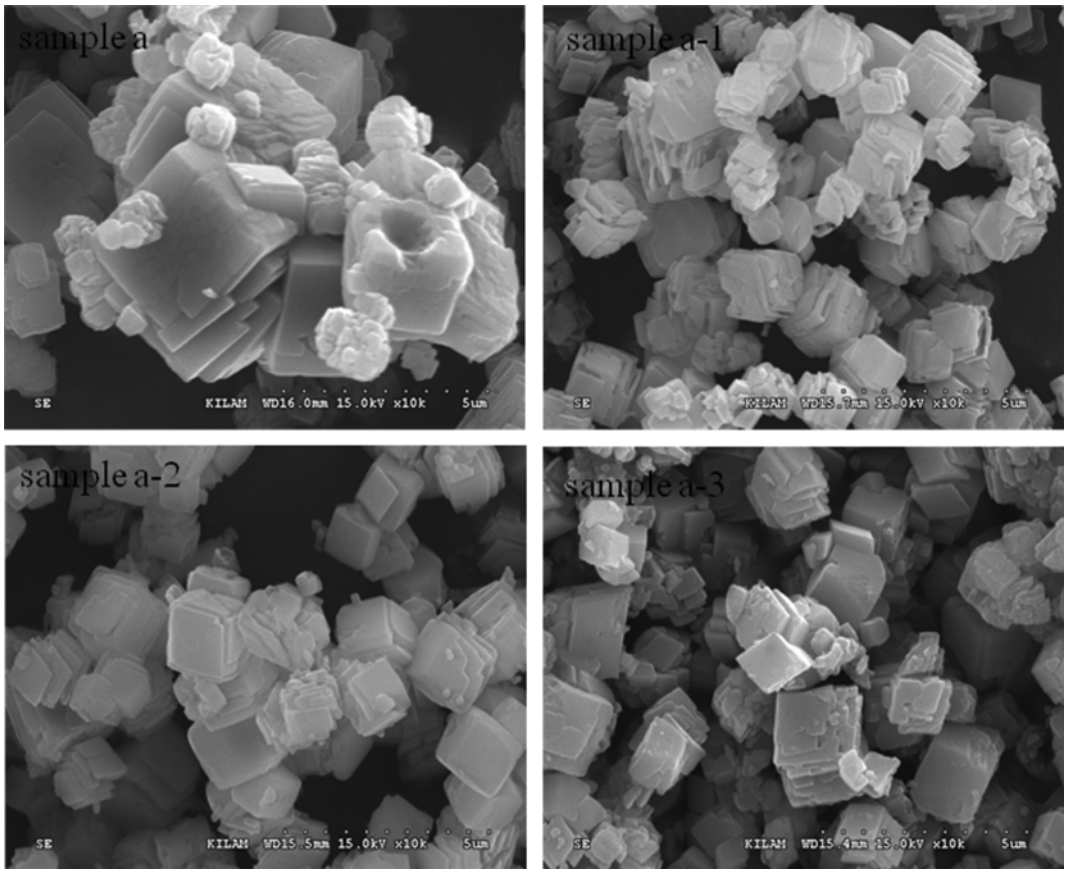

Fig. 2. SEM images of samples a (room temp.), a-1 (40 °C), a-2 (60 °C), a-3 (80 °C) (pH=9, $CaCl_2$: Na_2CO_3 1 : 1 molar ratio).

The syntheses were performed at pH 9, and a 1 : 1 mol ratio of $CaCl_2$ and Na_2CO_3. Temperatures ranged from room temperature to 80 °C. SEM images of the samples indicate that they were not affected by temperature: all formed the most stable structure, cubic calcite (Fig. 2) [2,7-9]. XRD analysis confirmed their calcite structures (Fig. 6). However, vaterite $CaCO_3$ has been reported from $CaCl_2$-Na_2CO_3 systems [31-37]. The sudden mixing of $CaCl_2$ and Na_2CO_3 with agitation for 30 s at room temperature followed by their undisturbed settling for 10 to 15 minutes can form amorphous, spherical, micro-crystals slowly through the transformation of calcium carbonate. Through the physical or chemical adsorption of anionic or cationic electrolytes to these micro-spheres, proteins and other useful substances can be loaded. In particular, D. V. Volodkin [36] noted the instability of vaterite $CaCO_3$ through its recrystallization (>80%) to the calcite structure in aqueous solution over 24 hrs. In the same work vaterite $CaCO_3$ was stabilized by electrolyte (PAH/PSS)$_3$ and could withstand storage for one week at room temperature. This indicates that cores formed through volume disorder by PSS of $Ca(R\text{-}SO_3)_2$ and CO_3^{2-} ion through reaction with $R\text{-}SO_3^-$ (Fig. 4).

Results indicated that the crystal morphology of calcium carbonate was not affected by temperature. On the other hand, the cluster size was affected by temperature (d_{50}=3.35 μm at 40 °C, d_{50}=4.41 μm at 80 °C).

2. The Effect of Anionic Surfactant on $CaCO_3$ Synthesis

2-1. Effects of SDBS on the Morphology of $CaCO_3$

Equimolar ratio $CaCl_2$ and Na_2CO_3 systems for $CaCO_3$ synthesis were tested with various amounts of SDBS additive from 0.003 to 1 mol with the aim of synthesizing vaterite $CaCO_3$ through its controlled crystallization using limestone. A low molecular weight anionic surfactant was used for this, whose structure is similar to that of the anionic electrolyte PSS [38-41]. Samples' SEM images are shown in Fig. 3 and indicate that sample b (0.003 mol SDBS) was calcite $CaCO_3$, similar to sample a, and that samples b-1 (0.01 mol SDBS), b-2 (0.1 mol SDBS) and b-3 (0.5 mol) exihibited both calcite and vaterite structures. With anionic surfactant, white $Ca(C_{12}H_{25}C_6H_4SO_3)_2$ formed through the reaction of Ca^{2+} and CO_3^{2-} ions with the SDBS, while calcite and vaterite $CaCO_3$ formed through the reaction of Ca^{2+} and CO_3^{2-} ions with Na_2CO_3. In sample b-4 (1.0 mol SDBS) $CaCO_3$ was synthesized with a hollow, vaterite structure. Thus hollow, spherical $CaCO_3$ vaterite structures were created through the formation of cores by the reaction of Ca^{2+} : $C_{12}H_{25}C_6H_4SO_3Na$: CO_3^{2-} with $CaCO_3$ core grains gathering by volume disorder from the surfactant's covalent electrons. This process showed similar results to the vaterite $CaCO_3$ synthesis reported by D. V. Volodkin that employed PSS rather than SDBS [36].

Vaterite structures crystallize in various ways and can become rose-shaped with growth in the x, y and z directions. Vaterite structures' crystallization can depend on the type of functional group (SO_3^-). The SEM images of samples b-2 (0.1 mol SDBS) and b-3 (0.5 mol SDBS) show their rose-shaped structures (Fig. 3) [39]. This kind of structure is believed due to the hydrophobic property of SDBS. The hydrophobic interaction between SDBS-plates might result in different angles and grow into rose-shaped.

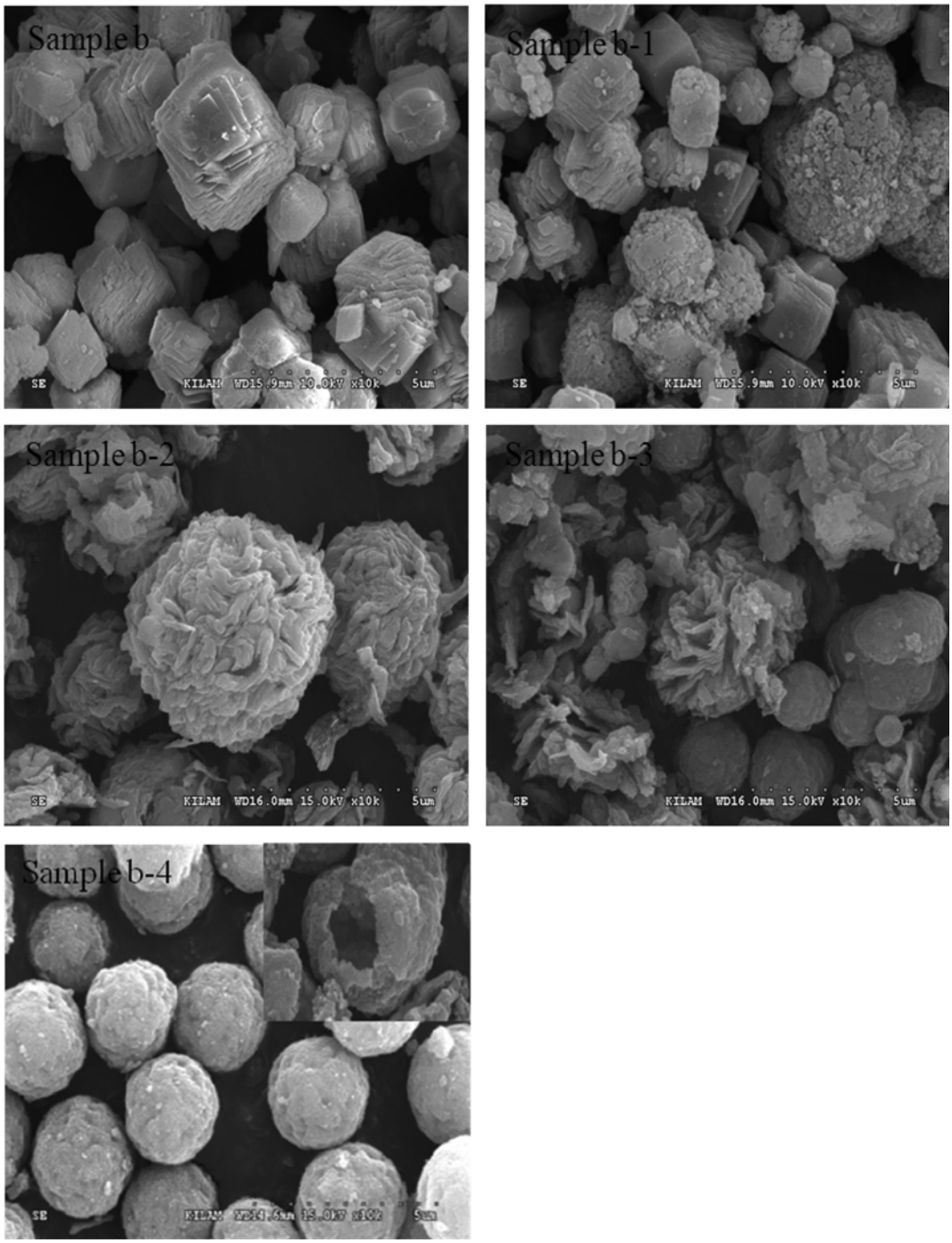

Fig. 3. SEM images of samples b (0.003 mol SDBS), b-1 (0.01 mol SDBS), b-2 (0.1 mol SDBS), b-3 (0.5 mol SDBS), b-4 (1 mol SDBS) (pH=9, $CaCl_2$: SDBS : Na_2CO_3 (1 : 1 molar ratio)).

XRD analysis of the b-series (without b-7, Fig. 7) also shows that with increasing concentration of anionic surfactant, a transfer from calcite to vaterite structures occurred. As sample b-4 was found to be of vaterite structure, it was subjected to further quantitative XRD analysis (Fig. 9), which found hollow $CaCO_3$ structures of 1.5% calcite and 98.5% vaterite.

Fig. 12 shows results of FT-IR analysis of samples, b to b-5 with $CaCO_3$ vibrational frequencies of CO_3^{2-} ions. The following peaks were observed for the samples: b, calcite (713, 1,426 cm^{-1}) and vaterite (878 cm^{-1}); b-1, calcite (712, 1,434 cm^{-1}) and vaterite (877 cm^{-1}); b-2 calcite (712, 1,426 cm^{-1}) and vaterite (878 cm^{-1}); b-3, calcite (713, 1,426 cm^{-1}) and vaterite (745, 878 cm^{-1}); b-4, calcite (1,440 cm^{-1}) and vaterite (745, 877 cm^{-1}). The figure also indicates the to The SEM images of Fig. 3, the XRD analysis of Fig. 7 and the XRD quantitative analysis of Fig. 9 support the conclusion that an increase of anion surfactant facilitated the formation of $CaCO_3$ micro-particles, while maintaining their spherical shape through the volume disorder of the anion surfactant, which also stabilized them in aque-

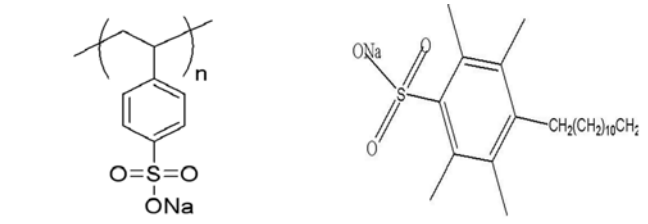

Fig. 4. Chemical structure of anionic polyelectrolyte (Poly(sodium 4-styrenesulfonate), left) and anionic surfactant (sodium dodecyl benzenesulfonic acid, right).

ous solutions.

2-2. Mechanism for the Crystallization of $CaCO_3$ with SDBS

Many researchers reported rose-shaped $CaCO_3$ with anionic surfactants [39,43-45]. Huang et al. [39] reported that the shape of $CaCO_3$ changed from monolayer to multilayer, and finally to rose-shaped type with SDSN as a surfactant. According to Matijevic group [43], rose-shaped vaterite was synthesized in urea solution (H_2NCONH_2) with SDSN and SDBS. They proposed that both preheating solution and increasing the concentration of urea offer more CO_3^{2-} and NH_4^+ through the hydrolysis of urea at 90 °C. It was reported that

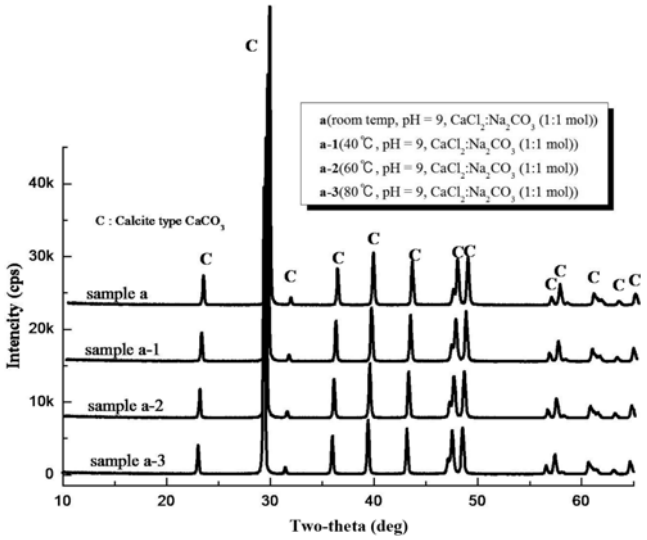

Fig. 6. XRD data of samples a (room temp), a-1 (40 °C), a-2 (60 °C), a-3 (80 °C) (pH=9, $CaCl_2$: Na_2CO_3 (1 : 1 molar ratio)).

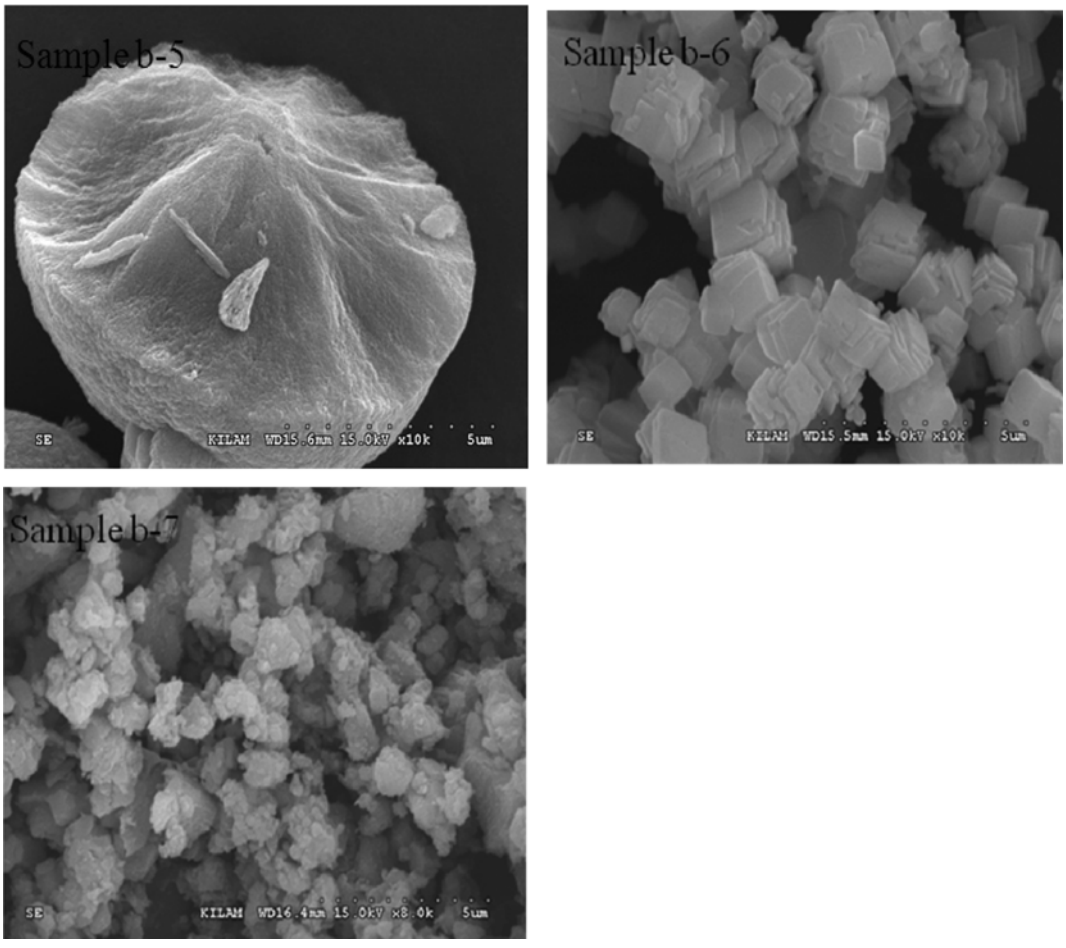

Fig. 5. SEM images of samples b-5 (1 mol SDBS), b-6 (no SDBS) (pH=9, $CaCl_2$: SDBS : Na_2CO_3 (1 : 1 molar ratio)) and b-7 ($Ca(OH)_2$, pH=9, $CaCl_2$: NaOH (1 : 2 molar ratio)).

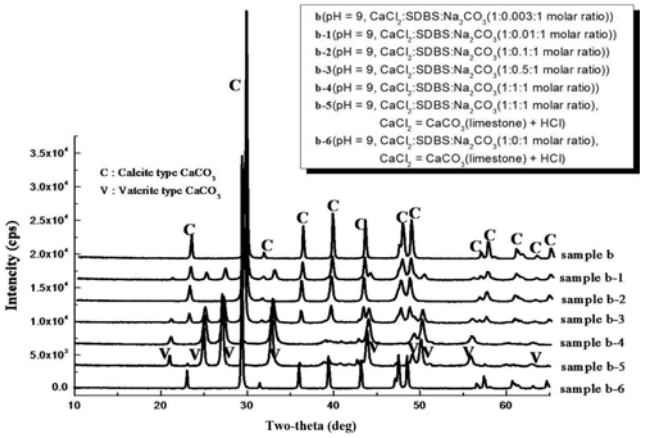

Fig. 7. XRD data analysis of sample b (0.003 mol SDBS), b-1 (0.01 mol SDBS), b-2 (0.1 mol SDBS), b-3 (0.5 mol SDBS), b-4 (1 mol SDBS), b-5 (1 mol SDBS), b-6 (no SDBS) (pH=9, $CaCl_2$: SDBS : Na_2CO_3 (1 : 1 molar ratio)).

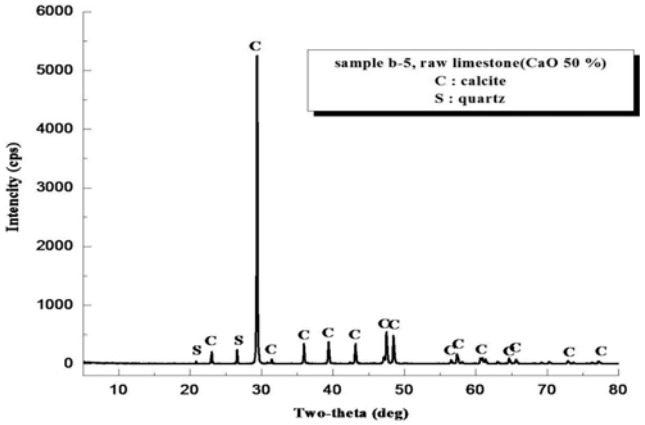

Fig. 8. XRD data analysis of limestone (sample b-5).

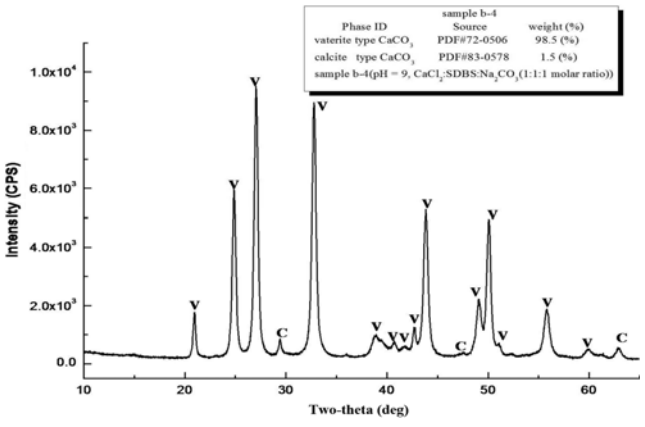

Fig. 9. XRD data and quantitative analysis of sample b-4 (pH=9, $CaCl_2$: SDBS : Na_2CO_3 (1 : 1 : 1 molar ratio)).

the formation of vaterite in aqueous solution was favored under conditions of high ratio of CO_3^{2-} : Ca^{2+} [44], and NH_4^+ can adsorb on the (001) faces of vaterite and act as a stabilizing agent [45]. Furthermore, CÖlfen's [45] recent research suggested that ammonium ions

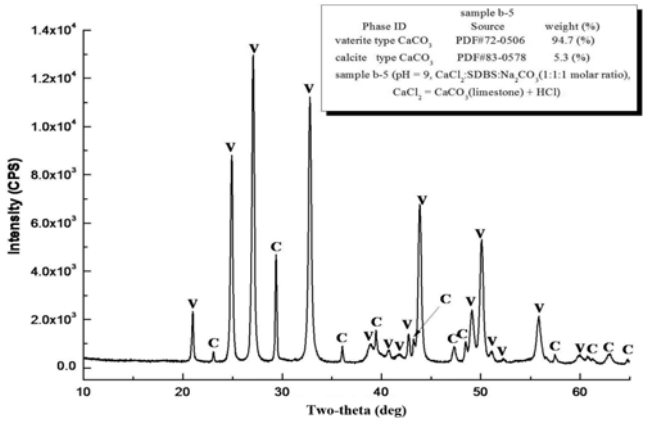

Fig. 10. XRD data and quantitative analysis of sample b-5 (pH=9, $CaCl_2$: SDBS : Na_2CO_3 (1 : 1 : 1 molar ratio)).

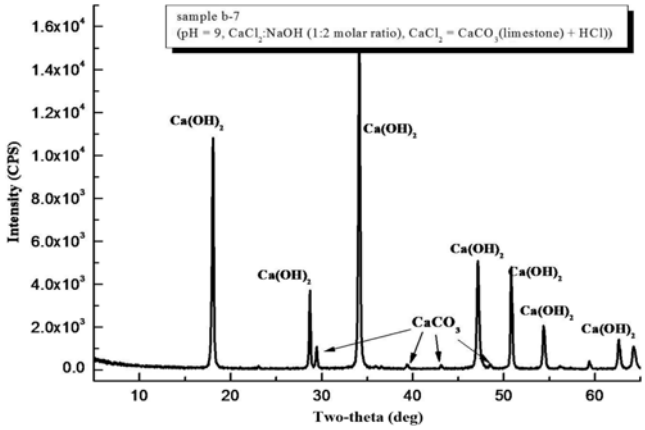

Fig. 11. XRD data of sample b-7 (pH=9, $CaCl_2$: NaOH (1 : 2 molar ratio)).

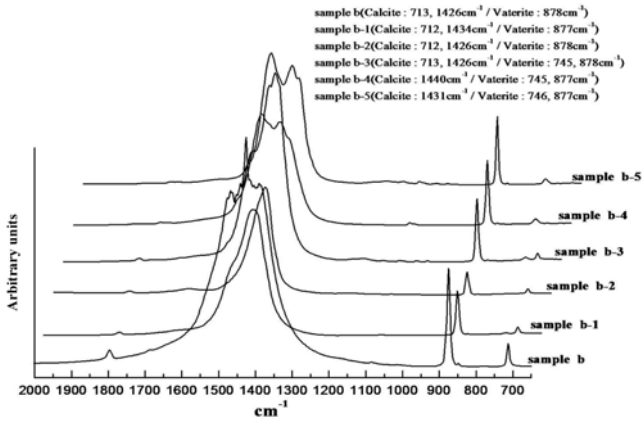

Fig. 12. FT-IR data of samples b, b-1, b-2, b-3, b-4, and b-5.

could play an important role in the formation of hexagonal vaterite.

In the presence of SDSN, hydrophobic interactions [46] between surfactant molecules force the adjacent hexagonal plates to assemble together and these plates finally grow into petals in different layers. The more that monomers adsorb in the face, a hydrophobic interaction exists between hexagonal plates. In the presence of SDBS,

the hydrophobic interaction between plates, as well as coarse surfaces of the plate, make it possible that other plates can be mounted in it by different angles and grow into petals.

This is believed to be the mechanism that rose-shaped $CaCO_3$ was synthesized with SDBS in our experiments.

3. The Effect of Limestone on the Synthesis of $CaCO_3$

Limestone is generally used in the synthesis of $CaCO_3$ polymorphs through the following three reactions:

$$\text{Limestone } (CaCO_3) \xrightarrow{\Delta} CaO+CO_2(g) \quad (2)$$

$$CaO+H_2O \rightarrow Ca(OH)_2 \quad (3)$$

$$Ca(OH)_2+CO_2(g) \rightarrow CaCO_3 \quad (4)$$

Limestone is a carbonate mineral theoretically composed of 56% CaO and 44% CO_2. Eq. (2) describes the production of CaO in shaft or rotary kilns that calcinate limestone [6]. Non-metallic minerals generally contain 1-3% impurities, lowering CaO content to 53-55%. Such impurities comprise Al_2O_3, Fe_2O_3, MgO and SiO_2, and they affect $CaCO_3$ by remaining throughout its synthesis [5,6].

The Solvay process is described in the following expression:

$$\text{Limestone } (CaCO_3)+HCl \rightarrow CaCl_2+CO_2(g)+H_2O \quad (5)$$

This process can form vaterite $CaCO_3$ by producing $CaCl_2$ solution (through the hydrochloric acid) which can be subsequently by employed in the $CaCl_2$-Na_2CO_3 system.

The molar quantity of hydrochloric acid for the reaction with limestone was optimized by reacting 125 μm limestone particles with 6 M HCl, with impurities removed by filtering through glass fiber. Remaining impurities in the $CaCl_2$ solution were determined through the following reaction:

$$CaCl_2+2NaOH \rightarrow Ca(OH)_2+2NaCl \quad (6)$$

By mixing $CaCl_2$ and NaOH at a 1 : 2 molar ratio, the theoretic reaction molar ratio, $Ca(OH)_2$ (sample b-7) was produced. Fig. 8 shows XRD data of limestone (sample b-5), indicating that it was composed of calcite and quartz, an impurity. Fig. 11 shows the XRD analyses of sample b-7 (pH=9, $CaCl_2$: NaOH 1 : 2 molar ratio), indicating the lack of other impurities, with peaks from mainly $Ca(OH)_2$ and also $CaCO_3$. The existence of $CaCO_3$ was attributable to HCO_3^{2-} ions in the water. Table 1 shows the results of the XRF analyses of limestone and what remained after it reacted with 6 M HCl. In the table, the molecular weight of limestone became 50.2 after the subtraction of the molecular weight of CO_2(g) (44) from the 94.2 of CaO. Table 2 shows the results of XRF analysis of $Ca(OH)_2$ (sample b-7), indicating that CaO was 99.5%.

$CaCO_3$ of vaterite structure was synthesized using limestone with equimolar ratios of $CaCl_2$: anionic surfactant (SDBS) : Na_2CO_3, found through reactions using the surfactant. After the $CaCl_2$ solution and anionic surfactant were mixed, a white solid formed, and further mixing with Na_2CO_3 solution led to vaterite $CaCO_3$ forming. After NaOH was mixed into the produced $CaCl_2$ solution at a 2 : 1 molar ratio, $Ca(OH)_2$ (sample b-7) was produced.

Fig. 5 shows SEM images of samples b-5 (1 mol SDBS), b-6 (no SDBS) and b-7 ($Ca(OH)_2$). Sample b-5 had spherical vaterite structures of $CaCO_3$, different from those of sample b-4, that were filled rather than the hollow spheres of sample b-4. The $CaCl_2$ af-

Table 1. XRF analysis of limestone and the product of the 6 M HCl +limestone reaction

Sample component	Limestone (mass%)	Remaining impurity after reacting 6 M HCl+limestone (mass%)
F		0.393
Na_2O	0.019	0.272
MgO	0.871	0.941
Al_2O_3	0.77	19.6
SiO_2	1.86	56.0
P_2O_5	0.016	0.017
SO_3	0.049	0.72
Cl	1.208	7.48
K_2O	0.144	5.37
CaO	94.2	5.78
MnO	0.031	
TiO_2	0.047	0.899
V_2O_5		0.07
Cr_2O_3	0.023	0.13
Fe_2O_3	0.65	2.07
NiO		0.026
CuO		0.009
ZnO		0.042
SeO_2		0.003
Rb_2O		0.018
SrO	0.112	0.012
ZrO_2		0.041
Nb_2O_5		0.004
BaO		0.08
PbO		0.016
U_3O_8		0.007

Table 2. XRF analysis of $Ca(OH)_2$ (sample b-7)

XRF analysis result		
No.	Component	Result (mass%)
1	F	0.254
2	Na_2O	0.0252
3	MgO	0.0264
4	Al_2O_3	0.0025
5	SiO_2	0.0203
6	SO_3	0.0353
7	Cl	0.0972
8	CaO	99.5
9	SrO	0.0089
	Ig-loss	0.0302

Table 3. The vibrational frequencies of CO_3^{2-} ions of calcium carbonate minerals

Calcium carbonate minerals	Vibrational frequencies of CO_3^{2-} ion			
	γ_1 (cm^{-1})	γ_2 (cm^{-1})	γ_3 (cm^{-1})	γ_4 (cm^{-1})
Calcite [42]		857	1426	712
Aragonite [42]	1082	859	1485	712, 699
Vaterite [42]	1085, 1070	870, 850, 830	1490, 1420	750

fected the growth of $CaCO_3$ cores due to the slight amount of impurities remaining after the reaction of limestone and hydrochloric acid. It was reacted with NaOH to assay these remaining impurities, with the resulting $Ca(OH)_2$ (sample b-7) containing *ca.* 0.5% impurities of F (0.254%), Na_2O (0.0252), MgO (0.0264%), Al_2O_3 (0.0025%), SiO_2 (0.0203%), SO_3 (0.0353%), Cl (0.0972%), SrO (0.0089) and Ig-loss (0.0302%). Other synthesis conditions were the same as for the anionic surfactant treatment of sample b. Sample b-6 was found to be calcite $CaCO_3$, similar to sample a, when the $CaCl_2$ solution was used at room temperature without surfactant (Fig. 5). Fig. 5 also shows an SEM image of sample b-7 ($Ca(OH)_2$) synthesized from the $CaCl_2$ solution.

The XRD data in Fig. 7 show that sample b-5, like sample b-4, was vaterite $CaCO_3$, while sample b-6 was confirmed of calcite structure, like sample a. The XRD data and quantitative analysis of sample b-5, show it to be composed of 94.7% vaterite and 5.3% calcite (Fig. 10). Compared with sample b-4, sample b-5 was found to contain more calcite by 3.8 percentage points, likely due to the effect of impurities in the $CaCl_2$ solution. The FT-IR data, confirmed that sample b-5 was composed of calcite (1,431 cm^{-1}) and vaterite (746, 877 cm^{-1}) (Fig. 12) [42].

CONCLUSIONS

The crystalline phase $CaCO_3$ in a $CaCl_2$-Na_2CO_3 system was controlled by adding surfactant. Without surfactant, calcite $CaCO_3$ was synthesized at pH 9 with equimolar reactant amounts of the theoretic reaction ratio. Although the crystal morphology of $CaCO_3$ was not affected, the cluster size was affected by temperature changes. Vaterite $CaCO_3$ was found to form in the presence of anionic surfactant (SDBS) under similar conditions where commercial $CaCl_2$ (purity >74%) was supplied. And XRD analysis found hollow vaterite structures accounting for up to 98.5% of the $CaCO_3$.

$CaCl_2$ solution was produced through the decomposition of limestone with hydrochloric acid using the Solvay process. The produced $CaCl_2$ solution was used in the $CaCl_2$-Na_2CO_3 system with and without added surfactant. XRD analysis showed that vaterite structures accounted for 94.7% of the $CaCO_3$ formed in this way in the presence of surfactant, with the remainder calcite. These vaterite structures were solid spheres rather than hollow ones.

Limestone was shown to be potentially useful in protein encapsulation by PSS, an anionic electrolyte, and PAH, a cationic electrolyte, in $CaCl_2$-Na_2CO_3 systems. $CaCO_3$ synthesized employing Solvay process and SDBS in this study can be used for such purpose.

REFERENCES

1. J. Perić, M. Vuèak and R. Krstuloviæ, *Thermochim. Acta*, **277**, 175 (1996).
2. M. S. Rao, *Bulletin Chem. Soc. Japan*, **46**, 1414 (1973).
3. L. F. Wang, I. Sondi and E. Matijeviæ, *J. Colloid Interface Sci.*, **218**, 545 (1999).
4. S. S. Berdonosov, I. V. Znamenskaya and I. V. Melikhov, *Inorganic Materials*, **41**(12), 1308 (2005).
5. J. G. Camona, J. G. Morales and R. R. Clemente, *J. Cryst. Growth*, **262**, 479 (2004).
6. A. M. Bes, *Process simulation of limestone calcination in normal shaft kilns*, Dr.-Ing. Thesis, Otto-von-Guericke University Magdeburg, Germany (2006).
7. J. Gómez-Morales, J. Torrent-Burgué and R. Rodríguez-Clemente, *J. Cryst. Growth*, **169**, 331 (1996).
8. C. Y. Tai and W. C. Chien, *Chem. Eng. Sci.*, **58**, 3233 (2003).
9. J. Kawano, N. Shimobayashi and M. Kitamura, *J. Cryst. Growth*, **237**, 419 (2002).
10. C. A. Bearchell, J. A. Edgar and D. M. Heyes, *J. Colloid Interface Sci.*, **210**, 231 (1999).
11. N. Wada, K. Kanamura and T. Umegaki, *J. Colloid Interface Sci.*, **233**, 65 (2001).
12. J. Yu, X. Zhao and B. Chenga, *J. Solid State Chem.*, **178**, 861 (2005).
13. K. J. Westin and Å. C. Rasmuson, *J. Colloid Interface Sci.*, **282**, 359 (2005).
14. K. J. Westin and Å. C. Rasmuson, *J. Colloid Interface Sci.*, **282**, 370 (2005).
15. W. Wu, T. He and J. Chen, *Mater. Lett.*, **60**, 2410 (2006).
16. J. Yu, M. Lei and B. Cheng, *J. Solid State Chem.*, **177**, 681 (2004).
17. Hua Tong, Wentao Ma and Leilei Wang, *Biomaterials*, **25**, 3923 (2004).
18. A. Xie, Y. Shen and C. Zhang, *J. Cryst. Growth*, **285**, 436 (2005).
19. N. Wada, K. Yamashita and T. Umegaki, *J. Colloid Interface Sci.*, **201**, 1 (1998).
20. I. Sondi and E. Matijeviæ, *J. Colloid Interface Sci.*, **238**, 208 (2001).
21. C. Jimenez-Lopez, A. Rodriguez-Navarro and J. M. Dominguez-Vera, *Geochimica et Cosmochimica Acta*, **67**(9), 1667 (2003).
22. S. Moya, L. Dähne and A. Voigt, *Colloids and Surfaces A*., **183**, 27 (2001).
23. A. A. Antipov and G. B. Sukhorukov, *Adv. Colloid Interface Sci.*, **111**, 49 (2004).
24. A. A. Antipov, G. B. Sukhorukov and S. Leporatti, *Colloids and Surfaces A*., **198**, 535 (2002).
25. G. Sukhorukov, A. Fery and H. Möhwald, *Prog. Polym. Sci*., **30**, 885 (2005).
26. Z. Dai, Andreas Voigt and S. Leporatti, *Adv. Mater*., **13**(17), 1339 (2001).
27. Z. Dai and H. Möhwald, *Langmuir*, **18**, 9533 (2002).
28. D. V. Volodkin, A. I. Petrov and M. Prevot, *Langmuir*, **20**, 3398 (2004).
29. T. Wang, H. Cölfen and M. Antonietti, *J. Am. Chem. Soc*., **127**, 3246 (2005).
30. G. Ibarz, L. Dähne and E. Donath, *Macromol. Rapid Commun*., **23**, 474 (2002).
31. C. W. Chengyi He and Z. Tong, *Int. J. Pharm.*, **308**, 160 (2006).
32. Y. Ueno, H. Futagawa and Y. Takagi, *J. Controlled Release*, **103**(1), 93 (2005).
33. D. V. Volodkin, A. I. Petrov and M. Prevot, *Langmuir*, **20**(8), 3398 (2004).
34. Q. Zhao, S. Zhang and W. Tong, *European Polym. J.*, **42**, 3341 (2006).
35. G. B. Sukhorukov, D. V. Volodkin and A. M. Günther, *J. Mater. Chem*., **14**, 2073 (2004).
36. D. V. Volodkin, N. I. Larionova and G. B. Sukhorukov, *Biomacromolecules*, **5**, 1962 (2004).
37. A. I. Petrov, D. V. Volodkin and G. B. Sukhorukov, *Biotechnol. Prog*., **21**, 918 (2005).

38. M. Lei, W. H. Tang and L. Z. Cao, *J. Cryst. Growth*, **294**, 358 (2006).
39. J. H. Huang, Z. F. Mao and M. F. Luo, *Mater. Res. Bull*, **42**(12), 2184 (2007).
40. H. Wei, Q. Shen and Y. Zhao, *J. Cryst. Growth*, **264**, 424 (2004).
41. H. Wei, Q. Shen and Y. Zhao, *J. Cryst. Growth*, **279**, 439 (2005).
42. W. Luo, *Infrared spectra of mineral*, Chongqing Scientific Publishing House, 55 (1988).
43. L. F. Wang, I. Sondi and E. Matijeviæ, *J. Colloid Interface Sci*., **545**, 218 (1999).
44. A. G. Turball, Geochin, *Cosmochim. Acta*., **1593**, 37 (1973).
45. N. Gehrke, H. CÖlfen and N. Pinna, *Cryst. Growth Des*., **1317**, 5 (2005).
46. M. Li, H. Schnablegger and S. Mann, *Nature*, **393**, 402 (1999).